NIH Public Access
Author Manuscript
Dev Biol. Author manuscript; available in PMC 2012 December 11.

Published in final edited form as:
Dev Biol. 2011 September 1; 357(1): 269–281. doi:10.1016/j.ydbio.2011.06.034.

Vgll2a is required for neural crest cell survival during zebrafish craniofacial development

Christopher W. Johnson[1,2], **Laura Hernandez-Lagunas**[1], **Weiguo Feng**[1,a], **Vida Senkus Melvin**[1], **Trevor Williams**[1], and **Kristin Bruk Artinger**[1,*]

[1]Department of Craniofacial Biology, University of Colorado Denver, School of Dental Medicine, Aurora, CO 80045, USA

[2]Molecular Biology Program, University of Colorado Denver, School of Dental Medicine, Aurora, CO 80045, USA

Abstract

Invertebrate and vertebrate vestigial (*vg*) and vestigial-like (*vgl*) genes are involved in embryonic patterning and cell fate determination. These genes encode cofactors that interact with members of the TEAD/Scalloped family of transcription factors and modulate their activity. We have previously shown that, in mice, *Vgll2* is differentially expressed in the developing facial prominences. In this study, we show that the zebrafish ortholog *vgll2a* is expressed in the pharyngeal endoderm and ectoderm surrounding the neural crest derived mesenchyme of the pharyngeal arches. Moreover, both the FGF and retinoic acid (RA) signaling pathways, which are critical components of the hierarchy controlling craniofacial patterning, regulate this domain of *vgll2a* expression. Consistent with these observations, *vgll2a* is required within the pharyngeal endoderm for NCC survival and pharyngeal cartilage development. Specifically, knockdown of Vgll2a in zebrafish embryos using Morpholino injection results in increased cell death within the pharyngeal arches, aberrant endodermal pouch morphogenesis, and hypoplastic cranial cartilages. Overall, our data reveal a novel non-cell autonomous role for Vgll2a in development of the NCC-derived vertebrate craniofacial skeleton.

Keywords

Vestigial-like; Vgl-2; VITO-1; craniofacial; zebrafish; FGF; Retinoic Acid; Cell Death

INTRODUCTION

The vertebrate craniofacial skeleton develops as a result of the specification, patterning, morphogenesis, and growth of tissues derived from all three germ layers in response to a complex network of reciprocal signaling (Chai and Maxson, 2006; Knight and Schilling, 2006). Ecto-mesenchymal neural crest cells (NCCs) are specified at the border between the neural and non-neural ectoderm and migrate ventro-laterally to populate the pharyngeal arches, a metameric series of bulges along the lateral surface of the developing head (Eisen

© 2011 Elsevier Inc. All rights reserved

[*]To whom all correspondence should be addressed T: 303-724-4562 | F: 303-724-4580 | Kristin.Artinger@ucdenver.edu.
[a]Present address: Stanford University, Cancer Center, Stanford, CA 94305

Publisher's Disclaimer: This is a PDF file of an unedited manuscript that has been accepted for publication. As a service to our customers we are providing this early version of the manuscript. The manuscript will undergo copyediting, typesetting, and review of the resulting proof before it is published in its final citable form. Please note that during the production process errors may be discovered which could affect the content, and all legal disclaimers that apply to the journal pertain.

$watermark-text
$watermark-text
$watermark-text

$watermark-text

$watermark-text

$watermark-text

and Weston, 1993; Le Douarin, 1982; Meulemans and Bronner-Fraser, 2004). The arches are separated from one another by pharyngeal pouches, invaginations of the endoderm lining the pharynx that contact the surface ectoderm of the embryo (Graham et al., 2005). Recent studies have demonstrated the importance of the pharyngeal endoderm and ectoderm in segmenting, patterning and promoting survival of the NCC-derived mesenchyme that, largely in response to these cues, gives rise to the pharyngeal skeleton. In the absence of the pharyngeal endoderm, as in the zebrafish *cas/sox32* mutant or as a result of physical ablation in chicken embryos, the pharyngeal cartilages fail to form (Couly et al., 2002; David et al., 2002). Specific factors expressed within the endoderm, such as TBX1, FGF3, FGF8, and EDN1, have also been shown to be important for cranial neural crest development (Arnold et al., 2006; Choudhry et al., 2010; David et al., 2002; Walshe and Mason, 2003). In addition, elements of the pharyngeal skeleton also fail to form in the absence of facial ectoderm (Hall, 1981) and expression of FGF8, EDN1, AP2a, SHH, TGF-β and WNT/β-catenin signaling in the ectoderm (Hu and Helms, 1999; Macatee et al., 2003; Nair et al., 2007; Reid et al., 2010; Xu et al., 2008) are important for proper gene expression and morphogenesis of the underlying NCC mesenchyme.

Our interest in identifying novel players in craniofacial development led us to perform a microarray screen aimed at identifying novel genes that are differentially expressed in the mouse face. One gene that was particularly enriched in the mandibular and maxillary prominences at embryonic day 10.5 was *vestigial-like 2* (*Vgll2*, also known as *VITO1* or *Vgl-2*), which encodes a member of the Vg-family of transcription cofactors. Members of this family are expressed in invertebrates and vertebrates and have been shown to be involved in a variety of developmental processes. In *Drosophila*, Vestigial (Vg) interacts with the transcription factor Scalloped (Sd) to regulate myogenesis and wing development (Bate and Rushton, 1993; Kim et al., 1996; Paumard-Rigal et al., 1998; Simmonds et al., 1998; Williams et al., 1991). The vertebrate Vg and Sd homologs, VGLL1-4 and TEAD1-4 respectively, contain conserved interaction domains and *in vitro* studies show that Vgll2 and Tead-1 (also known as TEF-1) physically interact via these domains (Chen et al., 2004; Gunther et al., 2004; Maeda et al., 2002). The interaction of Vgll2 and Tead-1 appears to play a role in skeletal muscle differentiation, modulating binding of Tead-1 to the MCAT recognition sequences and altering expression of myogenic genes. TEAD factors are broadly expressed during development and it is thought that more discrete expression of the interacting cofactors, such as *Vgll2*, confers tissue specificity to TEAD activity (Bonnet et al., 2010; Chen et al., 2004).

Vgll2 is expressed in a conserved pattern during development in all vertebrates examined. In the mouse, *Vgll2* is expressed beginning at embryonic day 8.0 (E8.0) in the pharyngeal arches and, by E9.5, in the myotomes of the somites and other sites of myogenesis (Maeda et al., 2002; Mielcarek et al., 2002). Expression of *VGLL2* is similar in chick and *Xenopus*, with the notable exception that it is also expressed in ventral domains within the brain in these organisms (Bonnet et al., 2010; Faucheux et al., 2010). The zebrafish genome contains two *VGLL2* orthologs, *vgll2a* and *vgll2b* (also known as *vgl-2a* and *vgl-2b*) (Mann et al., 2007). *vgll2b* is expressed in the notochord and developing skeletal muscle but expression within the pharyngeal arches has not been described (Mann et al., 2007).

Here we report that *vgll2a* is expressed in the pharyngeal endoderm and ectoderm in zebrafish. Injecting zebrafish embryos with antisense Morpholino oligonucleotides (MO) to reduce Vgll2a induces neural crest cell death within the pharyngeal arches at 24 hpf, resulting in hypoplasia of the pharyngeal skeleton. We also demonstrate that expression of *vgll2a* within the pharyngeal epithelia is regulated by FGFs and RA and may represent an intersection of these signaling pathways in regulating NCC survival and craniofacial development.

$watermark-text

$watermark-text

$watermark-text

MATERIALS AND METHODS

Animal maintenance

Zebrafish were maintained according to Westerfield (Westerfield, 2007) and staged according to Kimmel et al. (Kimmel et al., 1995). AB and TL wild-type lines were used. The p53 mutant fish line, *tp53*^{M214K}, has been previously described (Berghmans et al., 2005). *p53*$^{-/-}$ fish were obtained by incrossing *p53*$^{+/-}$ heterozygotes and genotyped by PCR with the forward primers 5'-AGCTGCATGGGGGGGAT-3' for the wild-type allele or 5'-AGCTGCATGGGGGGGAA-3' for the mutant allele and the reverse primer 5'-GATAGCCTAGTGCGAGCACACTCTT-3'. Genotyped *p53*$^{-/-}$ fish were then incrossed to obtain *p53*$^{-/-}$ embryos for experiments. The *sox10:egfp* (*Tg(−4.9sox10:egfp)*^{ba2}) line has also been previously described (Carney et al., 2006).

C57BL/6J mice (Jackson Labs) were maintained as previously described (Feng et al., 2009).

Knockdown of vgll2a

Vgll2a knockdown was completed by injecting embryos at the 1 to 4 cell-stage with a mixture of 2.5% fluorescein dextran (10,000 MW, lysine fixable, Invitrogen) and 5ng of antisense Morpholino oligonucleotides (MOs) with the sequence TTG GGT TGC ATC AGA GGC TTA C (*vgll2a* ATG MO), targeting the translation start site (Gene Tools, LLC). At 24 hpf, embryos were screened using a fluorescence stereomicroscope and only embryos with consistent fluorescein incorporation were used in subsequent analysis. To verify that the phenotypes observed in this morphant were the result of reduced Vgll2a rather than an off-target, embryos were also injected with a second Morpholino, TTG GGT TGC ATC AGA GGC TTA C (*vgll2a* e2i2 MO), targeting the second exon-intron splice junction of the mRNA. Targeting by this Morpholino is predicted to result in skipping of the second (TEAD interacting domain containing) exon during splicing of the *vgll2a* mRNA (Morcos, 2007). Translation of such a message should result in a frameshift mutation within exon three and a premature stop codon 102 nucleotides downstream of the initiating ATG. mRNA from 10 pooled, 24hpf embryos injected with 10ng *vgll2a* 2e2i MO or 10 uninjected embryos was isolated using the RNAeasy Micro Kit (Qiagen) and reverse transcribed into cDNA using the Superscript III First-Strand Synthesis System for RT-PCR (Invitrogen). RT-PCR of the entire *vgll2a* CDS was performed using this cDNA and forward primer 5'-ATG AGC TGC TTG GAT GTC ATG TAT C-3' and reverse primer 5'-TTA AAA CCA GTA CAA GTC CTT GCT C-3', while β-actin was amplified with forward primer 5'-CGA GCT GTC TTC CCA TCC A-3', and reverse primer 5'-TCA CCA ACG TAG CTG TCT TTC TG-3'. Interestingly, the expected incorrectly spliced *vgll2a* product was not observed, though the early stop codon associated with this message would likely result in its degradation by nonsense-mediated decay. Integrated densities for each band were measured using Adobe Photoshop CS3 (Adobe Systems Inc.) and the densities of *vgll2a* bands were normalized to the β-actin bands. This revealed that embryos injected with 10ng *vgll2a* 2e2i MO exhibited a 44% decrease in *vgll2a* message (Supplemental Figure 1B). Embryos injected with 10ng *vgll2a* 2e2i MO and stained for cartilage at 5 dpf exhibited similar craniofacial phenotypes as those embryos injected with the *vgll2a* ATG MO (compare Supplemental Figure 1A to Figure 2D), suggesting these MOs are likely both targeting *vgll2a.* Because the *vgll2a* ATG MO resulted in a stronger and more consistent phenotype at a lower dose, we used this morpholino for all subsequent knockdown experiments.

To further verify specificity of the *vgll2a* ATG MO, performed an experiment to rescue the cartilage phenotype observed in embryos injected with this MO by co-injection of *vgll2a* mRNA. A template for *vgll2a* mRNA was constructed by amplifying a ~875 bp fragment of the *vgll2a* cDNA from IMAGE cDNA clone 7452668 (Open Biosystems) using forward

$watermark-text

$watermark-text

$watermark-text

primer 5'-GAT CCT CGA GCC ACC ATG TCA TGT CTT GAC GTC ATG TAT CAA GTT TAT GGT CCA C-3', which has an altered sequence so this mRNA will not be targeted by the *vgll2a* ATG MO but still encodes the same amino acid sequence, and reverse primer 5'-GTT CTC TAG ATT ATT AAA ACC AGT ACA AGT CCT TGC TC-3'. The resulting product was cloned into pCR®II-TOPO® (Invitrogen). This clone was digested using Acc65I and SP6 polymerase was used to synthesize capped, polyadenylated mRNA using the mMESSAGE mMACHINE kit (Ambion). Injection of 100 pg of the resulting *vgll2aΔMO* mRNA caused no obvious developmental phenotype, but greater amounts resulted in severe edema, small or absent eyes, mild hypoplasia of the pharyngeal skeleton, and curved bodies (data not shown), most likely due to unregulated activity of Vgll2a. Embryos were injected as described above with either 6ng ATG MO alone or 6ng ATG MO along with 100pg *vgll2a*ΔMO mRNA injected at the one-cell stage. At 5 dpf we stained the cartilage of these larvae and counted the number of alcian-blue-positive pharyngeal cartilage elements that were observed (Supplemental Figure 2). While injection of 6ng *vgll2a* ATG MO alone resulted in a loss of almost all pharyngeal cartilages (Supplemental Figure 2B), co-injection with 100pg of *vgll2a*ΔMO mRNA resulted in the development of a greater number of pharyngeal cartilage elements (Supplemental Figure 2C,D). The partial rescue of the *vgll2a* morphant phenotype by con-injection with *vgll2a*ΔMO mRNA suggests that the *vgll2a* ATG MO specifically targets *vgll2a*.

To suppress p53 mediated, MO-induced cell death (Robu et al., 2007), all MO injections were carried out in $p53^{-/-}$ embryos with the exception of NCC migration analysis, in which *sox10:egfp* embryos were co-injected with 5 ng of the *vgll2a* ATG MO and 2 ng of p53 MO with the sequence 5'-GCG CCA TTG CTT TGC AAG AAT TG-3' (Gene Tools, LLC; Robu et al. 2007), and transplant experiments, which were conducted using wild-type embryos.

Skeletal staining

Cartilage was stained following Walker and Kimmel, 2007, with some modifications. 5 dpf larvae were fixed in 2% PFA for 1hr at room temperature, washed in 100mM Tris pH 7.5/10mM $MgCl_2$, and stained overnight in 0.04% alcian blue (Anatech Ltd) in 80% EtOH/100mM Tris pH 7.5/10mM $MgCl_2$. Larvae were then rehydrated in 80% EtOH/100mM Tris pH 7.5/10mM $MgCl_2$, followed by 50% and 25% EtOH/100mM Tris pH 7.5, washed in 3% H_2O_2/0.5% KOH to remove pigment, cleared in 25% glycerol/0.1% KOH, and stored in 50% glycerol/0.1% KOH.

Whole-mount in situ hybridization

Zebrafish whole-mount in situ hybridization (ISH) was adapted from Thisse and Thisse (Thisse and Thisse, 1998) and Brent and colleagues (Brent et al., 2003). BM Purple (Roche) was used as a substrate for the alkaline phosphatase reaction. A template for a *vgll2a* antisense riboprobe was constructed by amplifying a 871 bp fragment of the *vgll2a* cDNA from IMAGE cDNA clone 7452668 (Open Biosystems) using forward primer 5'-GCTGCTTGGATGTCATGTATCAAG-3' and reverse primer 5'-GTCCTTGCTCTTATCTTGGCTCTA-3'. The resulting product was cloned into pCR®IITOPO® (Invitrogen). This clone was digested using HindIII and T7 polymerase was used to synthesize an antisense probe to detect *vgll2a* expression. A template for *vgll2b* antisense riboprobe was constructed by cloning a 361 bp PvuII fragment isolated from IMAGE cDNA clone 7284235 (Open Biosystems) into pCR®-Blunt II-TOPO® (Invitrogen). This plasmid was digested with SpeI, and an antisense probe was synthesized using T7 polymerase. Other riboprobes used were *dlx2a* and *dlx5a* (Akimenko et al., 1994), *edn1* (Miller et al., 2000), *fgf3* (Maves et al., 2002), *fgf10a* (a gift from Dr. David Stock), *hand2* (Yelon et al., 2000), *nkx2.3* (Lee et al., 1996), *nkx3.2* (Miller et al., 2003), *shh* (Krauss et al., 1993), *sox9a* (Chiang et al., 2001), and *tbx1* (Piotrowski et al., 2003).

$watermark-text

$watermark-text

$watermark-text

For sectional analysis of *vgll2a* expression, after ISH, embryos were dehydrated through an ethanol series, embedded in JB-4 glycol methacrylate polymer (Polysciences Inc.) and sectioned at 4 μm using glass knives.

ISH of *Vgll2* in the mouse was performed as previously described (Feng et al., 2009).

Immunofluorescence

Embryos were fixed in 4% PFA for 1 hr at room temperature. For permeabilization, 24 and 48 hpf embryos were washed in distilled H_2O for 2 × 5 minutes, while 72 hpf embryos were washed for 5 minutes in distilled H_2O, 5 minutes in 100% acetone at -20°C, and another 5 minutes in distilled H_2O. Subsequent steps were carried out as described (Ungos et al., 2003). Primary antibodies used were zn-8 (anti-Alcama) (1:250; Developmental Studies Hybridoma Bank), anti-phospho-histone H3 (1:500; Millipore), and anti-active caspase-3 (1:250; BD Pharmingen), followed by Alexa Fluor® 488 or Alexa Fluor® 594 conjugated secondary antibodies (1:750; Molecular Probes).

Transplantations

Wild-type embryos were injected at the one-cell stage with 1ng *cas/sox32* mRNA (previously described, Dickmeis et al., 2001) synthesized with the mMESSAGE mMACHINE kit (Ambion) and 2.5% rhodamine dextran (tetramethylrhodamine dextran, 10,000 MW, lysine fixable, Invitrogen). At mid blastula stages, embryos were dechorionated and approximately 50 cells from the margin of these endodermally fated donor embryos were transplanted to the margin of wild-type embryos injected with 5 ng *vgll2a* ATG MO. At 30 hpf, embryos were screened using a fluorescence stereomicroscope and only those with pharyngeal endoderm-specific contribution of donor cells were used in subsequent analysis. At 5 dpf, embryos were fixed and cartilage was stained as described above.

Pharmacological treatments

At 22 hpf, manually dechorionated embryos were transferred into embryo media containing 20 μM SU5402 (3-[3-(2- carboxyethyl)-4-methylpyrrol-2-methylidenyl]-2-indolinone; CalBiochem; Mohammadi et al., 1997), 100 μM DEAB (4-(Diethylamino)benzaldehyde; Sigma-Aldrich), 100 nM all-*trans* retinoic acid (Sigma-Aldrich) or 0.2% DMSO as a carrier control and incubated at 28.5°C in the dark. After one hour, embryos were fixed in 4% PFA and processed by ISH.

Microarray

Mandibular, maxillary, and frontonasal prominences were collected at five time points between E10.5 and E12.5 from C57BL/6J (Jackson Labs) mouse embryos and analyzed by microarray using seven replicates for each sample as previously described (Feng et al., 2009).

Imaging and analysis

Processed embryos were mounted in glycerol and, for ISH and skeletal staining, imaged on a Zeiss Stemi SVII dissecting microscope or, for further magnification, an Olympus BX51WI compound microscope using a SPOT RT Slider camera and SPOT Software (Diagnostic Instruments, Inc.). ISH domains were measured using Adobe Photoshop CS3 (Adobe Systems Inc.).

For immunofluorescence, confocal images were captured on a Zeiss LSM 510 NLO using AxioVision software (Carl Zeiss). To quantify cell death and proliferation, Z stacks of 3μm confocal slices were analyzed using Imaris software (Bitplane Inc.).

$watermark-text

$watermark-text

$watermark-text

RESULTS

Previously, a microarray screen was performed comparing gene expression in the mouse mandibular, maxillary, and frontonasal prominences at five time points from embryonic day 10.5 (E10.5) to E12.5, during which these prominences undergo substantial growth, fusion, and morphogenesis (Feng et al., 2009). It was reasoned that genes differentially expressed in these samples might represent molecules with roles in these developmental processes. We were particularly interested in identifying those genes for which a role in orofacial development had not been described. One such gene identified in this screen was *vestigial-like 2* (*Vgll2*). In our microarray studies, we found that *Vgll2* expression was enriched in samples from the mandibular and maxillary prominences at E10.5 but not at later time points and not in samples from the frontonasal prominence (Supplemental Figure 3A). To confirm this finding, we performed RNA in situ hybridization (ISH) and found that *Vgll2* is expressed in the epithelia of the mandible and maxilla in the commissure of the developing mouth at E10.5 (Supplemental Figure 3B). We also found *Vgll2* to be expressed in the pharyngeal pouches and somites, as has been previously described (Maeda et al., 2002; Mielcarek et al., 2002). In order to determine the function of Vgll2 in craniofacial development, we utilized the zebrafish model and examined the expression of the two *Vgll2* homologs, *vgll2a* and *vgll2b*, to assess if transcripts derived from these genes were present in the facial complex.

vgll2a expression in the developing zebrafish

ISH analysis was used to examine expression of *vgll2a* in zebrafish at stages from 1-cell to 77 hours post fertilization (hpf). *vgll2a* is first expressed at the 2-somite stage (10.75 hpf) in the developing somites (Figure 1A), where it continues to be expressed throughout somitogenesis (Figure 1A–D). *vgll2a* is also faintly expressed in the notochord at these stages (data not shown). At 17 somites (17.5 hpf), *vgll2a* continues to be expressed in the somites (arrow) and begins to be expressed in discrete cell populations within the pharyngeal endoderm as they begin to evaginate to form the first endodermal pouch that separates arches one and two (Figure 1B, C). At 22 hpf (Figure 1D, E), expression of *vgll2a* is apparent in both the endoderm (black arrow) and ectoderm (white arrow) that surround the mesenchyme of the arches as they continue to develop in an anterior-posterior wave. At 30 hpf, expression of *vgll2a* was apparent in the region of the developing trigeminal ganglion (arrow; Figure 1F). Sectional analysis of embryos at 30 hpf confirmed that *vgll2a* is also prominently expressed in the pharyngeal endoderm and, to a lesser extent, the overlying ectoderm (Figure 1H–I). Expression of *vgll2a* was also apparent in the ventral forebrain (arrowheads Figure 1D and 1G) and this expression domain expands at later stages. Endodermal expression persists at later stages as the pouches continue their morphogenesis and fuse with the ectoderm to form gill slits between the arches (black arrow, Figure 1J–L). *vgll2a* begins to be expressed in the fin buds by 40 hpf (Figure 1J), in the developing cranial musculature by 48 hpf (Figure 1K) and at 64 hpf, *vgll2a* is re-expressed in the now mature somitic muscle (Figure 1L). Expression within the notochord was also apparent at later stages (arrowhead, Figure J–L). Like *Vgll2* in the mouse, *vgll2a* is also expressed in lateral edges of the stomodeum, the presumptive mouth, (white arrow, Figure 1J, Supplemental Figure 5A) and the commissure of the mouth after it opens (white arrow, Figure 1K–L, Supplemental Figure 5B).

Expression of the other zebrafish *VGLL2* paralog, *vgll2b*, has been previously examined at early stages (>24 hpf) and is observed in the notochord and somites in a pattern similar to *vgll2a*. We used ISH to examine expression of *vgll2b* at 24, 48, and 72 hpf and found that, unlike *vgll2a, vgll2b* is not expressed in the pharyngeal epithelia (Supplemental Figure 4). Other domains of expression appear to be relatively conserved between these paralogs at the stages analyzed.

$watermark-text

$watermark-text

$watermark-text

Our analysis shows that *vgll2a* and *vgll2b* are expressed in zebrafish in patterns similar to previously reported for *VGLL2* in other vertebrates (Bonnet et al., 2010; Faucheux et al., 2010; Maeda et al., 2002; Mielcarek et al., 2002). These data also provide support for a role for *vgll2a*, but not *vgll2b*, in the development of the pharyngeal skeleton.

vgll2a is required for cartilage development and endodermal pouch morphogenesis

To determine if *vgll2a* is required for development of the pharyngeal skeleton, we reduced Vgll2a function in zebrafish embryos using antisense Morpholino oligonucleotides (MO) targeting the translation start site of the message (*vgll2a* ATG MO) injected at the one to four cell stage. Following injection of 5 ng of *vgll2a* ATG MO, embryos exhibit a reduction in size of the overall jaw structure as compared with controls at 5 dpf (Figure 2A, B; n= 66/72). Alcian blue staining revealed hypoplasia or loss of cartilages of the viscerocranium in embryos injected with 5 ng *vgll2a* ATG MO relative to uninjected controls (Figure 2E,F). Cartilages derived from the first arch, Meckel's (m) and palatoquadrate (pq) cartilages, are severely hypoplastic in *vgll2a* morphants relative to uninjected controls (Figure 2C–F). This is also observed in second arch derivatives, including ceratohyal (ch) and hyosymplectic (hs) cartilages. Most of the skeletal derivatives of the posterior arches, the ceratobranchial (cb) cartilages, are absent (Figure 2E, F). The ethmoid plate of the neurocranium was also truncated in Morpholino injected animals relative to controls (Figure 2G, H). These data suggest that Vgll2a is required for craniofacial skeletal development in the zebrafish. While a more severe hypoplasia of the pharyngeal skeleton can be observed with injection of higher amounts of *vgll2a* ATG MO (see Supplemental Figure 2), in the interest of avoiding non-specific knockdown of off-target genes, we decided to perform experiments using the 5 ng dose.

The prominent expression of *vgll2a* within the pharyngeal endoderm led us to examine this tissue in *vgll2a* morphants. At 38 hpf, when all of the pouches have formed, we used the zn-8 antibody, which recognizes Alcama and is a marker of the pharyngeal endoderm (Choudhry et al., 2010; Fashena and Westerfield, 1999; Trevarrow et al., 1990), to visualize the pharyngeal pouches in morphant embryos and uninjected controls. The pharyngeal pouches of morphant embryos appeared shorter and wider than uninjected controls, suggesting that Vgll2a plays a role in morphogenesis of the endodermal pouches (Figure 3A, B). The presence of Alcama in the pouch endoderm as detected by the zn-8 antibody suggests that Vgll2a is not required for the specification of this tissue. To confirm proper specification of the pharyngeal endoderm, we examined the expression of genes including: *fgf3*, which is expressed in pharyngeal pouches at 24 hpf; *nkx2.3*, which is expressed in the pharyngeal endoderm and ectoderm surrounding the arches at 24 hpf; *end1*, which is expressed in the endoderm, ectoderm, and mesoderm of the arches at 24 hpf; *tbx1*, which is expressed in the pharyngeal endoderm and mesoderm at 30 hpf; and *shh*, which is expressed in pouch two and the oral ectoderm at 48 hpf (Supplemental Figure 6). Expression of these genes within the pharyngeal endoderm is essentially unchanged in *vgll2a* morphants relative to uninjected controls, providing further support for the proper specification of the pharyngeal epithelia when *vgll2a* is reduced. Together, these results suggest that Vgll2a is required for proper morphogenesis of the pharyngeal endoderm, but not for its specification.

Neural crest cell death within the arches is increased in *vgll2a* morphants

We next utilized ISH to determine how earlier defects in cranial NCCs might contribute to the hypoplastic cartilage defects in the Vgll2a morphants. We utilized probes specific for the homeodomain-containing transcription factors *dlx2a* at 24 hpf, when it is expressed in all NCCs of the pharyngeal arches (Figure 4A–B), and *barx1*, a marker of condensations of cranial NCCs as they undergo chondrogenesis, at 48 hpf (Figure 4D–E). While these genes were expressed in similar domains in uninjected and *vgll2a* MO injected embryos, the areas

$watermark-text

$watermark-text

$watermark-text

of the expression domains appeared reduced. To quantify this, we measured the area of each expression domain and compared the measurements from *vgll2a* morphants to those from uninjected embryos. All of the *dlx2a* domains measured are significantly smaller in *vgll2a* morphants (Figure 4C). Similarly, all of the *barx1* domains, with the exception of the ventral domain of arch 2, are also significantly smaller in morphants relative to uninjected controls (Figure 4F). Expression of *barx1* is notably absent in all but the most posterior ceratobranchial condensations of arches 3 – 5 in *vgll2a* morphants (bracket, Figure 4E).

To confirm proper specification of cranial NCCs we examined expression of genes normally expressed in arch NCCs, including *fgf10a, dlx5a, hand2, nkx3.2* (also known as *bapx1*), and *sox9a* at stages throughout development (Supplemental Figure 7). Like *dlx2a* and *barx1*, these genes are expressed in *vgll2a* morphants, but their domains of expression appear smaller in size relative to uninjected control embryos. Like *barx1*, however, *sox9a* appeared to be absent in the posterior arches. Together, these data suggest that while NCCs are generally specified and patterned correctly in *vgll2a* morphants, they appear reduced in number.

In order to determine if this reduction in NCCs within the arches might be attributed to a gross defect in the migration of these cells, we examined their migration in *sox10:egfp* transgenic embryos, which express EGFP specifically in NCCs. At 16, 17, and 18 hpf, we observed the three streams of cranial NCCs migrating into the aches as well as around the eye and into the frontonasal process of both uninjected and *vgll2a* morphant embryos (Supplemental Figure 8). There are no obvious differences in migration of cranial NCCs, suggesting that the decrease in the number of NCCs populating the arches of *vgll2a* morphants is not a result of earlier defects in migration. Together, these data suggest that, while NCCs are specified, migrate, and are patterned correctly in *vgll2a* morphants, they may be reduced in number.

We next determined if this reduction in cranial NCCs might be attributed to changes in proliferation or cell death. We used the zn-8 antibody to visualize the pharyngeal pouches and anti-phospho-histone H3 or anti-active caspase 3 to identify proliferating or apoptotic cells, respectively, at 24, 48, and 72 hpf. Within projected Z-stacks collected using confocal microscopy we modeled arch volumes in three dimensions based on zn-8 staining and found that the estimated arch volumes of *vgll2a* morphant embryos are smaller than those of uninjected controls (Supplemental Figure 9), which correlates with the observed reductions in NCC marker domains (Figure 4). Individual cells undergoing proliferation or apoptosis within the modeled arch volumes were counted and normalized for arch volume. Within these arch volumes, proliferation is unchanged in *vgll2a* morphants relative to uninjected controls at all three time points examined (Supplemental Figure 10). In contrast, cell death within the arches is increased seven-fold in *vgll2a* morphants at 24 hpf, but unchanged at 48 and 72 hpf (Figure 5). In order to confirm that the dying cells we observed within the arches of *vgll2a* morphants were indeed NCCs, we examined cell death using the anti-active caspase 3 antibody in *sox10:egfp* embryos that express egfp within the NCCs, and found that while there are no anti-caspase 3-positive cells within the arch NCCs of uninjected embryos at 24 hpf, dying NCCs can be seen within the arches of *vgll2a* MO injected embryos (Supplemental Figure 11). Together these data suggest that Vgll2a is required for survival of cranial NCCs within the arches at around 24 hpf and that the increased NCC cell death results in fewer NCCs populating the pharyngeal arches of *vgll2a* morphants.

Endodermal Vgll2a is sufficient for pharyngeal cartilage development

Because *vgll2a* is required for survival of neural crest cells within the arch, but is expressed most prominently in the pharyngeal endoderm, we hypothesized that Vgll2a is required

primarily within the pharyngeal endoderm for maintenance of NCCs and subsequent development of the pharyngeal cartilages.

To test this hypothesis, we transplanted *vgll2a* expressing cells into *vgll2a* morphant embryos and evaluated the ability of these cells to rescue development of the pharyngeal skeleton. At the blastoderm stage, cells at the margin of the embryo represent the presumptive mesendoderm (Kimmel et al., 1990). When transplanted to the margin of another embryo, however, these cells rarely contribute to the endoderm (Alexander et al., 1999; David and Rosa, 2001). In order for transplanted cells to contribute to the endoderm of mosaic embryos, donor embryos were fated to the endoderm lineage by injection with mRNA encoding *cas/sox32*, an endoderm specification protein (Chung and Stainier, 2008) at the one-cell stage (Figure 6A). Co-injection with the lineage tracer rhodamine dextran allowed us to identify transplanted cells at 30 hpf. Donor cells often contributed unilaterally to the pharyngeal endoderm of otherwise *vgll2a* morphant embryos (Figure 6B–C). By 5 dpf, these endodermally fated, wild type cells were able to partially or completely rescue development of the pharyngeal cartilages in 26% of these mosaic embryos (Figure 6D–G). In cases where these cartilages were not rescued by WT endodermal transplant, the number of transplanted cells contributing to the pharyngeal endoderm may not have been great enough to provide the number of *vgll2a*-expressing cells required for development of the adjacent cartilages. While these results suggest that the pharyngeal endoderm is a sufficient source of *vgll2a* for cartilage development to the extent we describe here, it is possible that expression of *vgll2a* within the overlying ectoderm normally contributes to craniofacial development. This result suggests that *vgll2a* is required primarily within the pharyngeal endoderm for development of the facial cartilages.

FGF and RA regulate Vgll2a expression within the pharyngeal epithelia

FGF and RA signaling pathways regulate endodermal pouch morphogenesis (Crump et al., 2004; Kopinke et al., 2006; Linville et al., 2009). FGFs are also required for survival of neural crest cells within the arches (Abu-Issa et al., 2002; Nissen et al., 2003; Trokovic et al., 2003; Yang et al., 2010) and both increased or reduced RA can result in cranial NCC apoptosis, suggesting a particular level of RA must be present to promote NCC survival (Begemann et al., 2001; Dickman et al., 1997; Sulik et al., 1988). Our finding that *vgll2a* is also important for these processes lead us to hypothesize that *vgll2a* might be regulated by FGFs and RA and act as an effector in these signaling pathways.

To test our hypothesis that *vgll2a* expression is regulated by FGF signaling, embryos were treated with SU5402, an inhibitor of the tyrosine kinase activity of FGF receptors (Mohammadi et al., 1997; Roehl and Nüsslein-Volhard, 2001), from 23 to 24 hpf. Treated embryos were then immediately fixed and analyzed by ISH to evaluate *vgll2a* expression. When compared to DMSO controls (Figure 7A), embryos treated with 20 μM SU5402 exhibit reduced expression of *vgll2a* within the pharyngeal epithelia (Figure 7B) while expression in other domains remains unaffected (data not shown). These data suggest that expression of *vgll2a* within the pharyngeal pouches is positively regulated by FGF signaling.

We also examined if *vgll2a* is regulated by RA by treating embryos from 22 to 23 hpf with 100 μM DEAB, an inhibitor of retinaldehyde dehydrogenase that reduces endogenous RA synthesis (Kopinke et al., 2006; Perz-Edwards et al., 2001) or 100 nM all-trans RA, and then assaying for *vgll2a* expression using ISH. Treatment with DEAB increases expression of *vgll2a* (Figure 7C) while treatment with RA results in decreased expression of *vgll2a* within the pharyngeal epithelia (Figure 7D). As with SU5402, neither treatment affects *vgll2a* expression in other domains (data not shown). Together these results demonstrate that RA negatively regulates vgll2a expression within the endodermal and ectodermal pharyngeal epithelia.

$watermark-text $watermark-text $watermark-text

$watermark-text

$watermark-text

$watermark-text

DISCUSSION

In this study, we have demonstrated a role for *vgll2a* in craniofacial development that is novel for *Vgl* family members. We have shown that *vgll2a* is expressed and required in the pharyngeal epithelia and that targeted knockdown of *vgll2a* leads to increased cell death within the arches and, subsequently, a reduction in the pharyngeal skeleton. Finally, we have reported that FGFs and RA, two signaling pathways that have been identified as important regulators of craniofacial development, also regulate expression of *vgll2a* in an opposing manner.

Evolutionary conservation of *vgll2a* and *vgll2b* expression

We have shown that in the developing zebrafish, *vgll2a* is expressed in the endodermal and ectodermal epithelia of the pharyngeal arches, as well as in the notochord, brain and sites of myogenesis. It's paralog, *vgll2b*, is expressed in a similar pattern but, unlike *vgll2a*, is not expressed in the pharyngeal arches. *VGLL2* is expressed in the arches of all other vertebrates examined (Bonnet et al., 2010; Faucheux et al., 2010; Maeda et al., 2002; Mann et al., 2007; Mielcarek et al., 2002), suggesting that *vgll2a* and *vgll2b* represent a case of genetic duplication and divergence. Some time after duplication during teleost evolution, *vgll2b* may have lost a cis-regulatory element driving expression with the pharyngeal arches. This similarities and differences in expression of *vgll2a* and *vgll2b* also imply that these paralogs may be functionally redundant in domains where both paralogs are expressed, such as the developing skeletal muscle, notochord, and brain, but that *vgll2a* acts independently from *vgll2b* in the development of the pharyngeal arches.

In the mouse, expression of *Vgll2* has been observed in the pharyngeal epithelia (Maeda et al., 2002; Mielcarek et al., 2002), but a functional, *in vivo* analysis has not been completed to date, making this study the first to do so in vertebrates. Although little has been described regarding the expression of human *VGLL2* gene, it is located at 6q21 (Maeda et al., 2002), within a 13 Mb region that has been linked to an autosomal recessive form of craniometaphyseal dysplasia, a disorder that causes, among other defects, hyperostosis of the bones of the face (Iughetti et al., 2000). Thus, it would be interesting to determine if VGLL2 plays a similar role in mammals and might contribute to the etiology of this disease.

vgll2a in cell death

Reduction of Vgll2a function results in hypoplasia of the facial cartilages. The remaining cartilaginous elements in *vgll2a* morphants, however, were patterned appropriately and markers for craniofacial development were generally expressed in the appropriate locations. While it is possible that NCCs are affected by other defects that we were unable to detect in our analysis, our data suggest that *vgll2a* does not play a role in migration, specification, or patterning of the cranial NCCs pharyngeal skeleton, but may be important for regulating cell number. In support of this idea, both the size of the craniofacial cartilages and the NCC marker domains were reduced in *vgll2a* morphants suggesting a change in NCC number. Indeed, we see an increase in apoptosis within the pharyngeal arches, but no change in cell proliferation, in *vgll2a* morphants. Together, these data suggest that *vgll2a* is required for maintenance of cranial NCC cells. While not all arch NCCs undergo apoptosis in embryos injected with 5 ng v*gll2a* ATG MO as was used in our analysis of cell death, it is likely that this dose does not result in complete knockdown of the gene. Indeed, injection with higher doses of v*gll2a* ATG MO resulted in stronger pharyngeal cartilage phenotypes (Supplemental Figure 2). As such, the *vgll2a* morphants described here probably do not reflect the full extent of cell death that might occur with complete knockdown of the gene.

$watermark-text

$watermark-text

$watermark-text

Cellular stress has also been shown to result in NCC death that can contribute to craniofacial phenotypes. Knockout of *polδ1* or *Tcof1* causes DNA damage leading to NCC apoptosis and, ultimately, craniofacial abnormalities (Jones et al., 2008; Plaster et al., 2006). In both cases, this apoptosis can be inhibited, and the craniofacial phenotypes effectively rescued, by the simultaneous attenuation of p53. Similarly, the non-specific apoptosis induced by injection of some morpholinos can also be eliminated by knockdown of p53 (Morcos, 2007). However, the cell death we observe in *vgll2a* morphants is p53-independent as these experiments were conducted in a $p53^{-/-}$ fish line, suggesting that the phenotypes we observe are not the result of cellular stress-induced apoptosis and supporting a role for *vgll2a* in regulating NCC survival.

The ability of *vgll2a*-expressing endoderm to rescue pharyngeal cartilage development in otherwise *vgll2a* morphant embryos supports *vgll2a* functioning to promote survival of cranial NCCs. We hypothesize that *vgll2a* regulates a survival signal originating from the pharyngeal endoderm and/or ectoderm that is required for NCC maintenance following migration into the pharyngeal arches. Similar mechanisms have been described in other vertebrate systems as a means of eliminating cells that have been mispatterned or otherwise strayed from their developmental path (Raff, 1992; Raff et al., 1994). The endoderm in particular has been shown to be a potent source of signals required for NCC survival; the zebrafish *casanova* (*cas/sox32*) mutant lacks all endoderm and exhibits cranial NCC death as a consequence (David et al., 2002).

We have described a novel role for *vgll2a* in promoting survival of NCCs. Our data demonstrate that *vgll2a* is required for neural crest cell survival within the arches at around 24 hpf, resulting in a reduction in cranial neural crest cell number in *vgll2a* morphants. Consequently, the anterior cartilage elements in embryos injected with 5 ng of *vgll2a* ATG MO are severely hypoplastic at 5 dpf when compared to controls. The absence of the ceratobranchial cartilages in these morphants may be due to a failure in the accumulation of enough NCCs to meet the critical mass required for chondrogenesis of these elements (Hall, 1987). Indeed, the posterior arches of *vgll2a* morphants failed to express *barx1* and *sox9a* during chondrogenesis. Neural crest cells that fail to undergo chondrogenesis but persist may remain undifferentiated and, subsequently, be eliminated in a second wave of cell death that occurs after 72 hpf, the last time point that we assayed.

Interestingly, the TEAD transcription factors have been shown to interact with the transcription co-activator YAP1 as part of the Hippo pathway, which controls organ size by regulating apoptosis and proliferation and has also been implicated in cancer (Goulev et al., 2008; Wu et al., 2008; Zhang et al., 2008; Zhao et al., 2010). It is possible that VGL, TEAD, and YAP1 function together to regulate hippo signaling, though this has not been examined. The *Drosophila* homologues of these proteins, however, have been shown to act together to regulate transcription (Goulev et al., 2008). The recent report that *yap1* knockdown by morpholino injection in zebrafish results in increased apoptosis and hypoplastic pharyngeal cartilages (Jiang et al., 2009) similar to the phenotypes we report here in *vgll2a* morphant embryos lends credence to the possibility that VGL, TEAD, and YAP1 function together in vertebrates as well. It is intriguing to consider the possibility, then, that the *vgll2a*-regulated survival signal is a Hippo target. Indeed, Hippo signaling has been shown to regulate the expression of many secreted growth factors and extracellular signaling molecules that would represent plausible candidates for such a survival signal (Hao et al., 2008; Zhang et al., 2011; Zhang et al., 2009; Zhao et al., 2008). It would be interesting to determine if such Hippo effectors are expressed in the pharyngeal epithelia, whether Vgll2a regulates their expression, and if they are required for neural crest survival.

$watermark-text

$watermark-text

$watermark-text

vgll2a regulation by FGF and RA

Opposing FGF and RA signals are a theme in the regulation of multiple events during embryonic development (Diez del Corral et al., 2003; Mercader et al., 2000). This paradigm may be reflected in our finding that expression of *vgll2a* within the pharyngeal epithelia, but not other domains of expression, is regulated positively by FGF and negatively by RA. In support of our data, expression of *Xenopus vgll2* is also responsive to FGF signaling in animal cap experiments (Faucheux et al., 2010). We have shown *vgll2a* expression is affected after modulating these signaling pathways for only 1 hour. The short time frame of these treatments suggests that *vgll2a* could be a direct transcriptional target of RA and FGF signaling and, as such, is inconsistent with the possibility that one signaling pathway might be affecting the activity of the other. We have also observed this regulation at 35 and 48 hpf (data not shown), demonstrating that FGF and RA regulate *vgll2a* expression within the pharyngeal arches throughout craniofacial development.

It is interesting to consider where the FGF and RA signals that regulate pharyngeal expression of *vgll2a* might originate. In zebrafish, *aldh1a2*, which encodes the retinaldehyde dehydrogenase responsible for RA synthesis, is expressed in the posterior arches at 24hpf (Vaccari et al., 2010; Wilm and Solnica-Krezel, 2005), when we have shown *vgll2a* to be regulated by RA. As such we believe this likely represents the source of RA that regulates expression within the pharyngeal epithelia. Given that there are at least 28 FGF ligands encoded by the zebrafish genome (Itoh, 2010), it is difficult to speculate about the source of the FGFs that drive pharyngeal expression of *vgll2a*. A number of studies have emphasized the importance of FGF8 in craniofacial development (Abu-Issa et al., 2002; Crump et al., 2004; Macatee et al., 2003), but we were unable to detect *fgf8* expression within the arches by ISH at 24 hpf (data not shown), when we have shown *vgll2a* to be regulated by FGF signaling. Fgf3 has also been shown to be important during craniofacial development and is expressed prominently within the pharyngeal pouches at 24 hpf (David et al., 2002; Walshe and Mason, 2003). Thus, we believe Fgf3 could represent an FGF source capable of regulating *vgll2a* expression. It is likely, however, that Fgf3 could act redundantly with one or more additional Fgf ligands such as Fgf8-related Fgf24, which is also expressed in the pharyngeal pouches (Jovelin et al., 2009; Mercader et al., 2006).

FGF has been implicated in NCC survival (Abu-Issa et al., 2002; Nissen et al., 2003; Trokovic et al., 2003; Yang et al., 2010) and cranial NCC death has been shown to result from an increase or decrease in RA (Begemann et al., 2001; Dickman et al., 1997; Sulik et al., 1988), which has been shown to regulate apoptosis in a myriad of ways (reviewed in Noy, 2010). As such, *vgll2a* could also be acting as an effector of FGF and/or RA signaling in the regulation of cell death. FGF and RA signaling have also been shown to regulate endodermal pouch morphogenesis (Crump et al., 2004; Kopinke et al., 2006; Linville et al., 2009). We first observe *vgll2a* expression in the pharyngeal endoderm in a subset of cells as they began to evaginate to form the first endodermal pouch and its expression in the pharyngeal endoderm persists throughout pouch morphogenesis. At 38 hpf, all of the endodermal pouches have formed, but in *vgll2a* morphants they appear shorter and wider than in uninjected embryos. This could suggest that *vgll2a* is required for endodermal pouch morphogenesis, perhaps by mediating the activity of FGF and/or RA signaling pathways. Interestingly, Vg has recently been shown to be required in *Drosophila* for cell shape changes in the developing wing disc pouch (Widmann and Dahmann, 2009), suggesting *vgll2a* could play an analogous role in pharyngeal pouch development. Alternatively, the aberration in endodermal pouch morphology could be secondary to the cranial NCC death that occurs in *vgll2a* morphants; the pouches may simply expand in the absence of physical constraint. Further experiments are required to determine how *vgll2a* affects pouch morphology.

In summary, we believe that *vgll2a* represents an important regulator of NCC survival during craniofacial development (Figure 8). Its expression within the pharyngeal epithelia is regulated positively by FGFs and negatively by RA and is required for survival of adjacent NCCs around 24 hpf. We postulate that at this time-point NCCs require a signal from the pharyngeal epithelia for their survival and that expression of this signal is regulated by *vgll2a* expression. Thus, in *vgll2a* morphants, a portion of these NCCs die, reducing the number of NCC cartilage progenitors and subsequently resulting in cartilage elements that are either reduced in size or absent, having failed to reach the critical mass required for chondrogenesis.

Supplementary Material

Refer to Web version on PubMed Central for supplementary material.

Acknowledgments

The authors would like to thank Sarah Wise and David Stock for help with sectioning and the gift of the *fgf10a* probe, Kristi LaMonica and Keith Anderson for help with confocal microscopy, Lee Niswander for use of her Imaris software, My Trang Nguyen for help with *vgll2b* expression, Morgan Singleton for fish care, Bruce Appel for the sharing the $tp53^{M214K}$ mutant fish line, and David Clouthier for critically reading the manuscript. We gratefully acknowledge the support of this research by NIH R21 DE018005 to T.W. and K.B.A., NIH R01 DE017699 to K.B.A, and NIH T32 GM08730 and NIH F31 DE19607 to C.W.J.

REFERENCES

Abu-Issa R, Smyth G, Smoak I, Yamamura K.-i. Meyers EN. Fgf8 is required for pharyngeal arch and cardiovascular development in the mouse. Development. 2002; 129:4613–4625. [PubMed: 12223417]

Akimenko MA, Ekker M, Wegner J, Lin W, Westerfield M. Combinatorial expression of three zebrafish genes related to distal-less: part of a homeobox gene code for the head. J Neurosci. 1994; 14:3475–3486. [PubMed: 7911517]

Alexander J, Rothenberg M, Henry GL, Stainier DY. casanova plays an early and essential role in endoderm formation in zebrafish. Dev Biol. 1999; 215:343–357. [PubMed: 10545242]

Arnold JS, Werling U, Braunstein EM, Liao J, Nowotschin S, Edelmann W, Hebert JM, Morrow BE. Inactivation of Tbx1 in the pharyngeal endoderm results in 22q11DS malformations. Development. 2006; 133:977–987. [PubMed: 16452092]

Bate M, Rushton E. Myogenesis and muscle patterning in Drosophila. C R Acad Sci III. 1993; 316:1047–1061. [PubMed: 8076205]

Begemann G, Schilling TF, Rauch GJ, Geisler R, Ingham PW. The zebrafish neckless mutation reveals a requirement for raldh2 in mesodermal signals that pattern the hindbrain. Development. 2001; 128:3081–3094. [PubMed: 11688558]

Berghmans S, Murphey R, Wienholds E, Neuberg D, Kutok J, Fletcher C, Morris J, Liu T, Schulte-Merker S, Kanki J. tp53 mutant zebrafish develop malignant peripheral nerve sheath tumors. Proc Natl Acad Sci USA. 2005; 102:407. [PubMed: 15630097]

Bonnet A, Dai F, Brand-Saberi B, Duprez D. Vestigial-like 2 acts downstream of MyoD activation and is associated with skeletal muscle differentiation in chick myogenesis. Mech Dev. 2010; 127:120–136. [PubMed: 19833199]

Brent AE, Schweitzer R, Tabin CJ. A somitic compartment of tendon progenitors. Cell. 2003; 113:235–248. [PubMed: 12705871]

Carney TJ, Dutton KA, Greenhill E, Delfino-Machín M, Dufourcq P, Blader P, Kelsh RN. A direct role for Sox10 in specification of neural crest-derived sensory neurons. Development. 2006; 133:4619–4630. [PubMed: 17065232]

Chai Y, Maxson RE. Recent advances in craniofacial morphogenesis. Dev Dyn. 2006; 235:2353–2375. [PubMed: 16680722]

$watermark-text $watermark-text $watermark-text

$watermark-text

$watermark-text

$watermark-text

Chen H, Maeda T, Mullett S, Stewart A. Transcription cofactor Vgl-2 is required for skeletal muscle differentiation. Dev Genet. 2004; 39:273–279.

Chiang EF, Pai CI, Wyatt M, Yan YL, Postlethwait J, Chung B. Two sox9 genes on duplicated zebrafish chromosomes: expression of similar transcription activators in distinct sites. Dev Biol. 2001; 231:149–163. [PubMed: 11180959]

Choudhry P, Joshi D, Funke B, Trede N. Alcama mediates Edn1 signaling during zebrafish cartilage morphogenesis. Dev Biol. 2010; 349:483–493. [PubMed: 21073867]

Chung W, Stainier D. Intra-Endodermal Interactions Are Required for Pancreatic β Cell Induction. Dev Cell. 2008; 14:582–593. [PubMed: 18410733]

Couly G, Creuzet S, Bennaceur S, Vincent C, Le Douarin NM. Interactions between Hox-negative cephalic neural crest cells and the foregut endoderm in patterning the facial skeleton in the vertebrate head. Development. 2002; 129:1061–1073. [PubMed: 11861488]

Crump JG, Maves L, Lawson ND, Weinstein BM, Kimmel CB. An essential role for Fgfs in endodermal pouch formation influences later craniofacial skeletal patterning. Development. 2004; 131:5703–5716. [PubMed: 15509770]

David NB, Rosa FM. Cell autonomous commitment to an endodermal fate and behaviour by activation of Nodal signalling. Development. 2001; 128:3937–3947. [PubMed: 11641218]

David NB, Saint-Etienne L, Tsang M, Schilling TF, Rosa FM. Requirement for endoderm and FGF3 in ventral head skeleton formation. Development. 2002; 129:4457–4468. [PubMed: 12223404]

Dickman ED, Thaller C, Smith SM. Temporally-regulated retinoic acid depletion produces specific neural crest, ocular and nervous system defects. Development. 1997; 124:3111–3121. [PubMed: 9272952]

Dickmeis T, Mourrain P, Saint-Etienne L, Fischer N, Aanstad P, Clark M, Strahle U, Rosa F. A crucial component of the endoderm formation pathway, CASANOVA, is encoded by a novel sox-related gene. Genes Dev. 2001; 15:1487–1492. [PubMed: 11410529]

Diez del Corral R, Olivera-Martinez I, Goriely A, Gale E, Maden M, Storey K. Opposing FGF and retinoid pathways control ventral neural pattern, neuronal differentiation, and segmentation during body axis extension. Neuron. 2003; 40:65–79. [PubMed: 14527434]

Eisen JS, Weston JA. Development of the neural crest in the zebrafish. Dev Biol. 1993; 159:50–59. [PubMed: 8365574]

Fashena D, Westerfield M. Secondary motoneuron axons localize DM-GRASP on their fasciculated segments. J Comp Neurol. 1999; 406:415–424. [PubMed: 10102505]

Faucheux C, Naye F, Treguer K, Fedou S, Thiebaud P, Theze N. Vestigial like gene family expression in Xenopus: common and divergent features with other vertebrates. J Dev Biol. 2010; 54:1375–1382.

Feng W, Leach SM, Tipney H, Phang T, Geraci M, Spritz RA, Hunter LE, Williams T. Spatial and temporal analysis of gene expression during growth and fusion of the mouse facial prominences. PLoS ONE. 2009; 4:e8066. [PubMed: 20016822]

Goulev Y, Fauny JD, Gonzalez-Marti B, Flagiello D, Silber J, Zider A. SCALLOPED interacts with YORKIE, the nuclear effector of the hippo tumor-suppressor pathway in Drosophila. Curr Biol. 2008; 18:435–441. [PubMed: 18313299]

Graham A, Okabe M, Quinlan R. The role of the endoderm in the development and evolution of the pharyngeal arches. J Anat. 2005; 207:479–487. [PubMed: 16313389]

Gunther S, Mielcarek M, Kruger M, Braun T. VITO-1 is an essential cofactor of TEF1-dependent muscle-specific gene regulation. Nucleic Acids Res. 2004; 32:791. [PubMed: 14762206]

Hall BK. The induction of neural crest-derived cartilage and bone by embryonic epithelia: an analysis of the mode of action of an epithelial-mesenchymal interaction. J Embryol Exp Morphol. 1981; 64:305–320. [PubMed: 7310307]

Hall BK. Sodium fluoride as an initiator of osteogenesis from embryonic mesenchyme in vitro. Bone. 1987; 8:111–116. [PubMed: 3593607]

Hao Y, Chun A, Cheung K, Rashidi B, Yang X. Tumor suppressor LATS1 is a negative regulator of oncogene YAP. J Biol Chem. 2008; 283:5496–5509. [PubMed: 18158288]

Hu D, Helms JA. The role of sonic hedgehog in normal and abnormal craniofacial morphogenesis. Development. 1999; 126:4873–4884. [PubMed: 10518503]

$watermark-text

$watermark-text

$watermark-text

Itoh N. Hormone-like (endocrine) Fgfs: their evolutionary history and roles in development, metabolism, and disease. Cell Tissue Res. 2010; 342:1–11. [PubMed: 20730630]

Iughetti P, Alonso LG, Wilcox W, Alonso N, Passos-Bueno MR. Mapping of the autosomal recessive (AR) craniometaphyseal dysplasia locus to chromosome region 6q21-22 and confirmation of genetic heterogeneity for mild AR spondylocostal dysplasia. Am J Med Genet. 2000; 95:482–491. [PubMed: 11146471]

Jiang Q, Liu D, Gong Y, Wang Y, Sun S, Gui Y, Song H. yap is required for the development of brain, eyes, and neural crest in zebrafish. Biochem Biophys Res Commun. 2009; 384:114–119. [PubMed: 19393221]

Jones NC, Lynn ML, Gaudenz K, Sakai D, Aoto K, Rey J-P, Glynn EF, Ellington L, Du C, Dixon J, Dixon MJ, Trainor PA. Prevention of the neurocristopathy Treacher Collins syndrome through inhibition of p53 function. Nat Med. 2008; 14:125–133. [PubMed: 18246078]

Jovelin R, Yan YL, He X, Catchen J, Amores A, Canestro C, Yokoi H, Postlethwait JH. Evolution of developmental regulation in the vertebrate FgfD subfamily. J Exp Zool B Mol Dev Evol. 2009; 314:33–56. [PubMed: 19562753]

Kim J, Sebring A, Esch JJ, Kraus ME, Vorwerk K, Magee J, Carroll SB. Integration of positional signals and regulation of wing formation and identity by Drosophila vestigial gene. Nature. 1996; 382:133–138. [PubMed: 8700202]

Kimmel C, Ballard W, Kimmel S, Ullmann B, Schilling T. Stages of embryonic development of the zebrafish. Dev Dyn. 1995; 203:253–310. [PubMed: 8589427]

Kimmel CB, Warga RM, Schilling TF. Origin and organization of the zebrafish fate map. Development. 1990; 108:581–594. [PubMed: 2387237]

Knight RD, Schilling TF. Cranial neural crest and development of the head skeleton. Adv Exp Med Biol. 2006; 589:120–133. [PubMed: 17076278]

Kopinke D, Sasine J, Swift J, Stephens WZ, Piotrowski T. Retinoic acid is required for endodermal pouch morphogenesis and not for pharyngeal endoderm specification. Dev Dyn. 2006; 235:2695–2709. [PubMed: 16871626]

Krauss S, Concordet JP, Ingham PW. A functionally conserved homolog of the Drosophila segment polarity gene hh is expressed in tissues with polarizing activity in zebrafish embryos. Cell. 1993; 75:1431–1444. [PubMed: 8269519]

Le Douarin, NM. The Neural Crest. Cambridge University Press; New York: 1982.

Lee KH, Xu Q, Breitbart RE. A new tinman-related gene, nkx2.7, anticipates the expression of nkx2.5 and nkx2.3 in zebrafish heart and pharyngeal endoderm. Dev Biol. 1996; 180:722–731. [PubMed: 8954740]

Linville A, Radtke K, Waxman JS, Yelon D, Schilling TF. Combinatorial roles for zebrafish retinoic acid receptors in the hindbrain, limbs and pharyngeal arches. Dev Biol. 2009; 325:60–70. [PubMed: 18929555]

Macatee TL, Hammond BP, Arenkiel BR, Francis L, Frank DU, Moon AM. Ablation of specific expression domains reveals discrete functions of ectoderm- and endoderm-derived FGF8 during cardiovascular and pharyngeal development. Development. 2003; 130:6361–6374. [PubMed: 14623825]

Maeda T, Chapman D, Stewart A. Mammalian vestigial-like 2, a cofactor of TEF-1 and MEF2 transcription factors that promotes skeletal muscle differentiation. J Biol Chem. 2002; 277:48889. [PubMed: 12376544]

Mann CJ, Osborn DPS, Hughes SM. Vestigial-like-2b (VITO-1b) and Tead-3a (Tef-5a) expression in zebrafish skeletal muscle, brain and notochord. Gene Expr Patterns. 2007; 7:827–836. [PubMed: 17916448]

Maves L, Jackman W, Kimmel CB. FGF3 and FGF8 mediate a rhombomere 4 signaling activity in the zebrafish hindbrain. Development. 2002; 129:3825–3837. [PubMed: 12135921]

Mercader N, Fischer S, Neumann CJ. Prdm1 acts downstream of a sequential RA, Wnt and Fgf signaling cascade during zebrafish forelimb induction. Development. 2006; 133:2805–2815. [PubMed: 16790478]

$watermark-text

$watermark-text

$watermark-text

Mercader N, Leonardo E, Piedra ME, Martínez-A C, Ros MA, Torres M. Opposing RA and FGF signals control proximodistal vertebrate limb development through regulation of Meis genes. Development. 2000; 127:3961–3970. [PubMed: 10952894]

Meulemans D, Bronner-Fraser M. Gene-regulatory interactions in neural crest evolution and development. Dev Cell. 2004; 7:291–299. [PubMed: 15363405]

Mielcarek M, Günther S, Krüger M, Braun T. VITO-1, a novel vestigial related protein is predominantly expressed in the skeletal muscle lineage. Mech Dev. 2002; 119:269–274.

Miller C, Schilling T, Lee K, Parker J, Kimmel C. sucker encodes a zebrafish Endothelin-1 required for ventral pharyngeal arch development. Development. 2000; 127:3815–3828. [PubMed: 10934026]

Miller CT, Yelon D, Stainier DYR, Kimmel CB. Two endothelin 1 effectors, hand2 and bapx1, pattern ventral pharyngeal cartilage and the jaw joint. Development. 2003; 130:1353–1365. [PubMed: 12588851]

Mohammadi M, McMahon G, Sun L, Tang C, Hirth P, Yeh BK, Hubbard SR, Schlessinger J. Structures of the tyrosine kinase domain of fibroblast growth factor receptor in complex with inhibitors. Science. 1997; 276:955–960. [PubMed: 9139660]

Morcos P. Achieving targeted and quantifiable alteration of mRNA splicing with Morpholino oligos. Biochem Biophys Res Commun. 2007; 358:521–527. [PubMed: 17493584]

Nair S, Li W, Cornell R, Schilling TF. Requirements for Endothelin type-A receptors and Endothelin-1 signaling in the facial ectoderm for the patterning of skeletogenic neural crest cells in zebrafish. Development. 2007; 134:335–345. [PubMed: 17166927]

Nissen RM, Yan J, Amsterdam A, Hopkins N, Burgess SM. Zebrafish foxi one modulates cellular responses to Fgf signaling required for the integrity of ear and jaw patterning. Development. 2003; 130:2543–2554. [PubMed: 12702667]

Noy N. Between death and survival: retinoic acid in regulation of apoptosis. Annu. Rev. Nutr. 2010; 30:201–217. [PubMed: 20415582]

Paumard-Rigal S, Zider A, Vaudin P, Silber J. Specific interactions between vestigial and scalloped are required to promote wing tissue proliferation in Drosophila melanogaster. Dev Genes Evol. 1998; 208:440–446. [PubMed: 9799424]

Perz-Edwards A, Hardison NL, Linney E. Retinoic acid-mediated gene expression in transgenic reporter zebrafish. Dev Biol. 2001; 229:89–101. [PubMed: 11133156]

Piotrowski T, Ahn D.-g. Schilling TF, Nair S, Ruvinsky I, Geisler R, Rauch G-J, Haffter P, Zon LI, Zhou Y, Foott H, Dawid IB, Ho RK. The zebrafish van gogh mutation disrupts tbx1, which is involved in the DiGeorge deletion syndrome in humans. Development. 2003; 130:5043–5052. [PubMed: 12952905]

Plaster N, Sonntag C, Busse CE, Hammerschmidt M. p53 deficiency rescues apoptosis and differentiation of multiple cell types in zebrafish flathead mutants deficient for zygotic DNA polymerase delta1. Cell Death Differ. 2006; 13:223–235. [PubMed: 16096653]

Raff MC. Social controls on cell survival and cell death. Nature. 1992; 356:397–400. [PubMed: 1557121]

Raff MC, Barres BA, Burne JF, Coles HS, Ishizaki Y, Jacobson MD. Programmed cell death and the control of cell survival. Philos Trans R Soc Lond, B, Biol Sci. 1994; 345:265–268. [PubMed: 7846124]

Reid BS, Yang H, Melvin VS, Taketo MM, Williams T. Ectodermal WNT/β-catenin signaling shapes the mouse face. Dev Biol. 2010

Robu M, Larson J, Nasevicius A, Beiraghi S, Brenner C, Farber S, Ekker S. p53 activation by knockdown technologies. PLoS Genet. 2007; 3:e78. [PubMed: 17530925]

Roehl H, Nüsslein-Volhard C. Zebrafish pea3 and erm are general targets of FGF8 signaling. Curr Biol. 2001; 11:503–507. [PubMed: 11413000]

Simmonds AJ, Liu X, Soanes KH, Krause HM, Irvine KD, Bell JB. Molecular interactions between Vestigial and Scalloped promote wing formation in Drosophila. Genes Dev. 1998; 12:3815–3820. [PubMed: 9869635]

Sulik KK, Cook CS, Webster WS. Teratogens and craniofacial malformations: relationships to cell death. Development. 1988; 103(Suppl):213–231. [PubMed: 3074910]

$watermark-text

$watermark-text

$watermark-text

Thisse C, Thisse B. High resolution whole-mount in situ hybridization. The Zebrafish Science Monitor. 1998; 5:8–9.

Trevarrow B, Marks DL, Kimmel CB. Organization of hindbrain segments in the zebrafish embryo. Neuron. 1990; 4:669–679. [PubMed: 2344406]

Trokovic N, Trokovic R, Mai P, Partanen J. Fgfr1 regulates patterning of the pharyngeal region. Genes Dev. 2003; 17:141–153. [PubMed: 12514106]

Ungos JM, Karlstrom RO, Raible DW. Hedgehog signaling is directly required for the development of zebrafish dorsal root ganglia neurons. Development. 2003; 130:5351–5362. [PubMed: 13129844]

Vaccari E, Deflorian G, Bernardi E, Pauls S, Tiso N, Bortolussi M, Argenton F. prep1.2 and aldh1a2 participate to a positive loop required for branchial arches development in zebrafish. Dev Biol. 2010; 343:94–103. [PubMed: 20423710]

Walshe J, Mason I. Fgf signalling is required for formation of cartilage in the head. Dev Biol. 2003; 264:522–536. [PubMed: 14651935]

Westerfield, M. A guide for the laboratory use of zebrafish (Danio rerio). 5th ed.. Univ. of Oregon Press; Eugene: 2007. The zebrafish book.

Widmann TJ, Dahmann C. Wingless signaling and the control of cell shape in Drosophila wing imaginal discs. Dev Biol. 2009; 334:161–173. [PubMed: 19627985]

Williams JA, Bell JB, Carroll SB. Control of Drosophila wing and haltere development by the nuclear vestigial gene product. Genes Dev. 1991; 5:2481–2495. [PubMed: 1752439]

Wilm TP, Solnica-Krezel L. Essential roles of a zebrafish prdm1/blimp1 homolog in embryo patterning and organogenesis. Development. 2005; 132:393–404. [PubMed: 15623803]

Wu S, Liu Y, Zheng Y, Dong J, Pan D. The TEAD/TEF family protein Scalloped mediates transcriptional output of the Hippo growth-regulatory pathway. Dev Cell. 2008; 14:388–398. [PubMed: 18258486]

Xu X, Han J, Ito Y, Bringas P, Deng C, Chai Y. Ectodermal Smad4 and p38 MAPK are functionally redundant in mediating TGF-beta/BMP signaling during tooth and palate development. Dev Cell. 2008; 15:322–329. [PubMed: 18694570]

Yang X, Kilgallen S, Andreeva V, Spicer DB, Pinz I, Friesel R. Conditional expression of Spry1 in neural crest causes craniofacial and cardiac defects. BMC Dev Biol. 2010; 10:48. [PubMed: 20459789]

Yelon D, Ticho B, Halpern ME, Ruvinsky I, Ho RK, Silver LM, Stainier DY. The bHLH transcription factor hand2 plays parallel roles in zebrafish heart and pectoral fin development. Development. 2000; 127:2573–2582. [PubMed: 10821756]

Zhang H, Pasolli HA, Fuchs E. Yes-associated protein (YAP) transcriptional coactivator functions in balancing growth and differentiation in skin. Proc Natl Acad Sci USA. 2011; 108:2270–2275. [PubMed: 21262812]

Zhang J, Ji JY, Yu M, Overholtzer M, Smolen GA, Wang R, Brugge JS, Dyson NJ, Haber DA. YAP-dependent induction of amphiregulin identifies a non-cell-autonomous component of the Hippo pathway. Nat Cell Biol. 2009; 11:1444–1450. [PubMed: 19935651]

Zhang L, Ren F, Zhang Q, Chen Y, Wang B, Jiang J. The TEAD/TEF family of transcription factor Scalloped mediates Hippo signaling in organ size control. Dev Cell. 2008; 14:377–387. [PubMed: 18258485]

Zhao B, Li L, Lei Q, Guan KL. The Hippo-YAP pathway in organ size control and tumorigenesis: an updated version. Genes Dev. 2010; 24:862–874. [PubMed: 20439427]

Zhao B, Ye X, Yu J, Li L, Li W, Li S, Lin JD, Wang CY, Chinnaiyan AM, Lai ZC, Guan KL. TEAD mediates YAP-dependent gene induction and growth control. Genes Dev. 2008; 22:1962–1971. [PubMed: 18579750]

$watermark-text

$watermark-text

$watermark-text

Research Highlights

- *vgll2a* is expressed in the pharyngeal endoderm and ectoderm surrounding the neural crest derived mesenchyme of the pharyngeal arches.
- FGF and retinoic acid (RA) signaling pathways regulate this domain of *vgll2a* expression.
- *vgll2a* is required within the pharyngeal epithelia for NCC survival and development of the cranial cartilages.
- These data reveal a novel non-cell autonomous role for Vgll2a in development of the NCC-derived vertebrate craniofacial skeleton.

$watermark-text
$watermark-text
$watermark-text

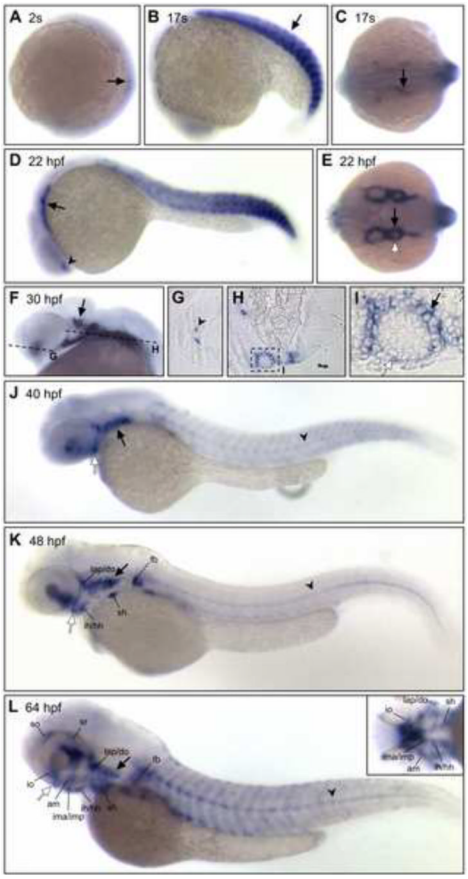

Figure 1. *vgll2a* expression in the developing zebrafish

In situ hybridization (ISH) using a *vgll2a* probe at 2 somites (A), 17 somites (B, C), 22 hpf (D, E), 30 hpf (F–I), 40 hpf (J), 48 hpf (K) and 64 hpf (L) stages showing lateral (A, B, D, F, J, K, L), dorsal (C, E) or ventral (inset, L) views. 4μm plastic sections (G, H, I) of 30 hpf embryos sectioned in planes shown in panel F. *vgll2a* is first detected in the developing somites (black arrows, A and B) of zebrafish at the 2-somite stage (A). By 17 somites (B,C), *vgll2a* is also expressed at low levels in a population of endodermal cells (black arrow, C) as they evaginate to form the first pharyngeal pouch. At 22 hpf, lateral (D) and dorsal (E) views reveal that *vgll2a* is also expressed in the lateral pharyngeal endoderm (black arrows, D, E) as the pouches continue to form, as well as in the ventral forebrain (black arrowhead, D). At 30 hpf, expression of *vgll2a* is also apparent in the region of the developing trigeminal ganglion (black arrow, F; dashed lines indicate plane of section in G–I). 4 μm plastic sections of 30 hpf embryos (G, H, I) reveal that vgll2a expression, in addition to being expressed within a discrete population of cells within the ventral forebrain (black arrowhead, G) and prominently in the pharyngeal pouch endoderm (H, and black arrow in higher magnification view of boxed region in, I), is also expressed in the overlying pharyngeal ectoderm (white arrow, I). From 30 to 48 hpf (F–K), *vgll2a* continues to be expressed in the endodermal pouches (black arrow, J), somite expression fades, and forebrain expression expands. At 40 hpf and later stages, *vgll2a* is expressed in the stomodeum, the presumptive mouth (white arrow, J, K, L). By 48 hpf (K), it begins to be expressed in sites of myogenesis other than the somites, including the fin bud (fb) and cephalic musculature and is also apparent in the notochord (black arrowhead). Cranial muscle expression is more apparent by 64 hpf (L), at which time *vgll2a* becomes reactivated in the somitic muscle. Anterior is to the left in all panels. am, adductor mandibulae; do,

dilator operculi; hh, hyohyoideus; ih, interhyoideus; ima, intermandibularis anterior; imp, intermandibularis posterior; io, inferior oblique; lap, levator arcus palatini; sh, sternohyoideus; so, superior oblique; sr, superior rectus.

$watermark-text

$watermark-text

$watermark-text

$watermark-text
$watermark-text
$watermark-text

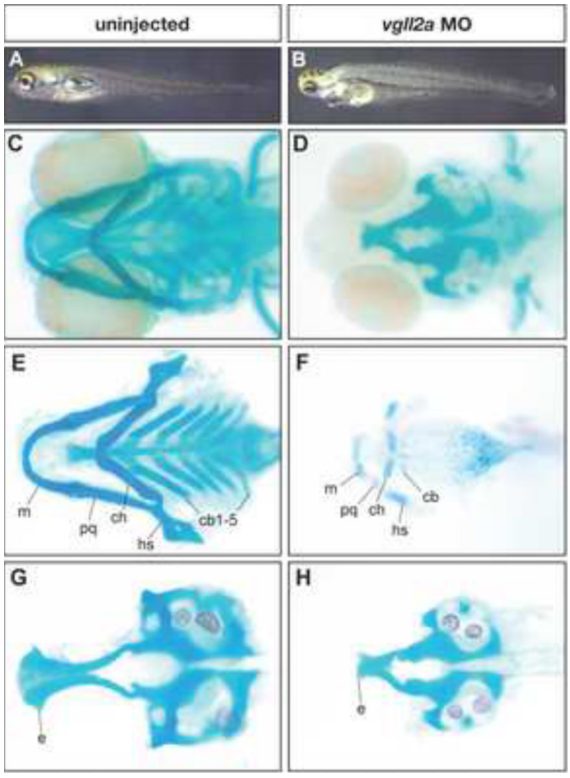

Figure 2. Pharyngeal cartilage development is affected in *vgll2a* morphants

Uninjected (A,C,E,G) and *vgll2a* morphant (B,D,F,H) embryos at 5 dpf (A,B) and alcian blue staining of these embryos (C–H) in whole mount (C,D), and after dissection to isolate the viscerocranium (E,F) and neurocranium (G,H). A typical embryo injected with 5 ng *vgll2a* ATG morpholino (B) exhibits a reduction in jaw structure relative to an uninjected control (A). Staining of the cranial cartilages with alcian blue in whole mount (C–D) and in dissected embryos (E–H) reveals the absence of the ceratobranchials 1–5 and hypoplastic Meckel's, palatoquadrate, ceratohyal and hyosymplectic cartilages in *vgll2a* morphants (F) relative to uninjected controls (E). Additionally, the anterior part of the neurocranium, the ethmoid plate, is truncated in *vgll2a* morphants (H) relative to controls (G). Anterior is to the left in all panels. e, ethmoid plate; cb, ceratobranchial; ch, ceratohyal; hs, hyosymplectic; m, Meckel's cartilage; pq, palatoquadrate.

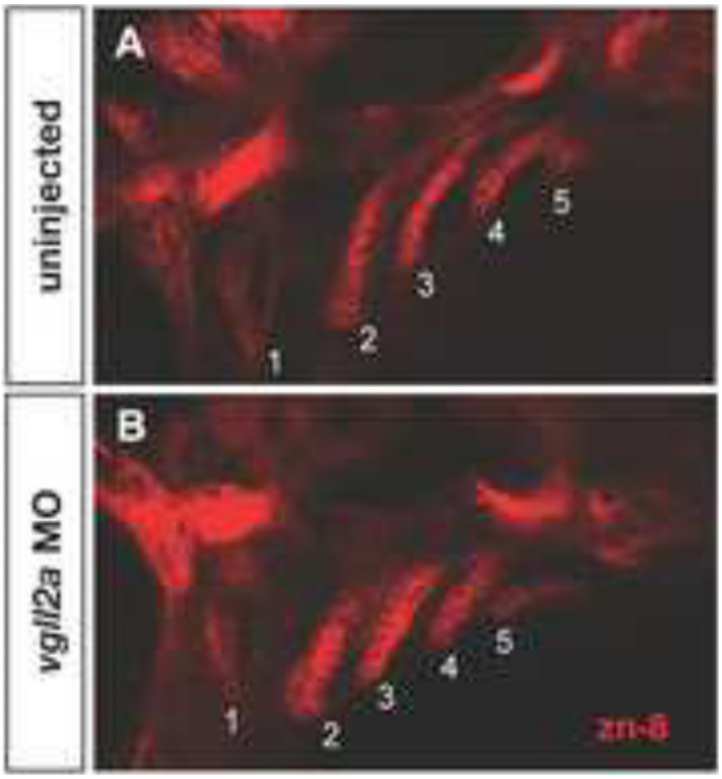

Figure 3. Endodermal pouch morphogenesis is affected in *vgll2a* morphants

Single confocal, Z-plane images of an uninjected (A) and *vgll2a* morphant embryo (B), stained with the zn-8 antibody, marking the endodermal pouches in lateral views. Uninjected embryos (A) exhibit elongated endodermal pouches, numbered 1 – 5, formed by tight folds of epithelium at 38 hpf. In contrast, the endodermal pouches of embryos injected with 5 ng *vgll2a* ATG MO (B) are shorter and wider, and the epithelial cells appear less organized relative to uninjected controls. Anterior is to the left in both panels.

$watermark-text
$watermark-text
$watermark-text

$watermark-text
$watermark-text
$watermark-text

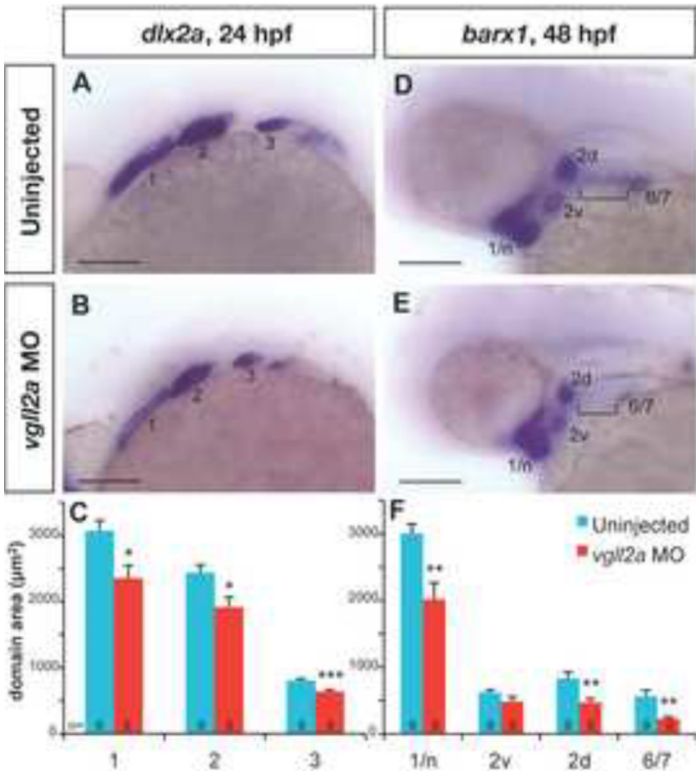

Figure 4. *vgll2a* knockdown causes a reduction in the size of NCC domains

Later views of uninjected (A,D) and *vgll2a* morphant (B,E) embryos processed by ISH with probes for *dlx2a* at 24 hpf (A,B) and *barx1* at 48 hpf (D,E). Dotted lines outlined in panels A,B,D and E represent the domain areas quantified (C,F). The domains of NCC marker *dlx2a* (A,B) in the first three arches (numbered 1–3) are smaller in *vgll2a* morphants (B) relative to uninjected controls (A) at 24 hpf. *barx1* is expressed in cranial NCC condensations at 48 hpf (D,E) and expression domains including the neurocranium and arch 1 (1/n), dorsal and ventral domains within arch 2 (2d and 2v) and a domain representing arches 6 and 7 (6/7) are similarly reduced in vgll2a morphants (E) relative to controls (D). *barx1* expression in the anterior ceratobranchials (bracket, D,E) was not detected in *vgll2a* morphant embryos (E). Graphs of the average area in these embryos reflect these differences (C, F). Error bars represent standard error of the mean. All domains measured were significantly smaller in *vgll2a* morphants except 2v (Student's T Test,*: $p < 0.05$, **: $p < 0.01$, ***: $p < 0.001$). Scare bars = 100 μm. Numbers at the base of each bar represent the number of embryos counted for each condition.

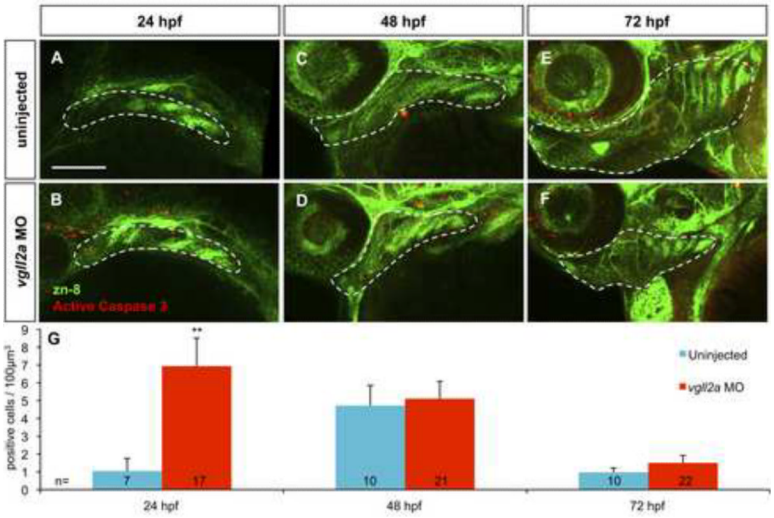

Figure 5. Cell death within the pharyngeal arches is increased in *vgll2a* morphants

Three-dimensional projections of confocal slices of representative uninjected (A,C,E) and *vgll2a* morphant embryos (B,D,F) at 24 (A,B) 48 (C,D) and 72 hpf (E,F) stained with zn-8 (anti-Alcama) and anti-activated caspase 3 antibodies in lateral views, and quantification of cell death in uninjected and morphant embryos (G). Embryos injected with 5ng *vgll2a* ATG MO (B,D,F) exhibit a greater number of activated caspase 3 positive cells (red) per μm^3 within arches volumes modeled within the white dashed lines based on zn-8 staining (green) relative to uninjected controls (A, C, E), at 24, but not 48 or 72 hpf. (G) Quantification of the average number of active caspase 3 positive cells / 100 μm^3 of arch volume per embryo (Student's T Test, **: $p < 0.01$). Error bars represent standard error of the mean. Numbers at the base of each bar represent the number of embryos counted for each condition. Scale bar = 100 μm.

$watermark-text
$watermark-text
$watermark-text

$watermark-text

$watermark-text

$watermark-text

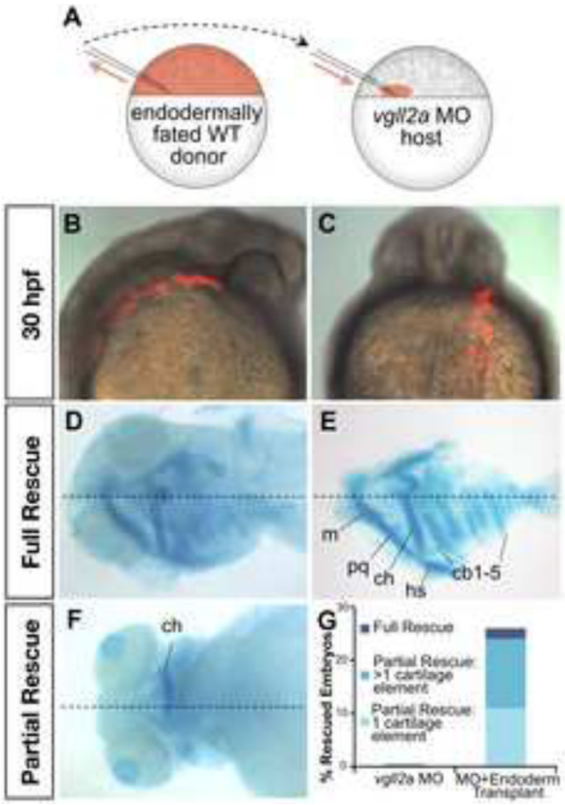

Figure 6. Expression of *vgll2a* in the pharyngeal endoderm is sufficient for facial cartilage development

Schematic representation of transplantation performed with endodermally fated wildtype *vgll2* expressing (WT) cells (A). To create mosaic embryos that express *vgll2a* within the pharyngeal endoderm but are otherwise *vgll2a* knockdown in all other cells, donor embryos were injected at the single-cell stage with *cas/sox32* mRNA to fate these embryos to become endoderm along with a rhodamine-dextran tracer. At blastoderm stage, cells were transplanted from the margin of these endodermally fated donor embryos to the margin of *vgll2a* morphant embryos (A). Lateral (B, anterior is to the right) and posterior (C) views of a representative mosaic embryo at 30 hpf following transplantation, these cells appear red by fluorescent microscopy and often contribute to one side of the pharyngeal endoderm and can be seen in lateral (B) and dorsoposterior (C) views. Ventral view at 5 dpf, alcian blue staining revealed that pharyngeal cartilage development is completely (wholemount, D, and dissected, E) or partially (F) rescued in some of these embryos. Quantification of number *vgll2a* morphant embryos that exhibited rescue upon introduction of endoderm from embryos expressing *vgll2a* (G). Rescue was scored as rescue of one cartilage element, rescue of more than one cartilage element, or rescue of all cartilage elements (full rescue) relative to morphants and expressed as a percent of the total number of mosaic embryos analyzed (G, n=46). 26% of endoderm transplants showed partial or full rescue. Dotted lines mark the approximate midline. cb, ceratobranchial; ch, ceratohyal; hs, hyosymplectic; m, Meckel's cartilage; pq, palatoquadrate.

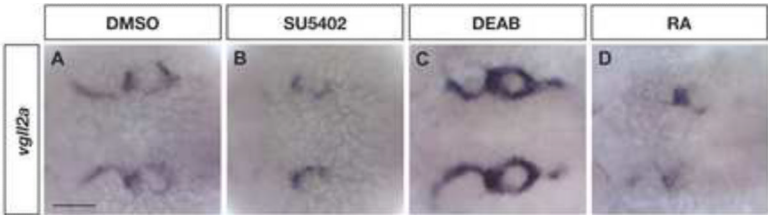

Figure 7. Expression of *vgll2a* is regulated by FGF and RA signaling

Dorsal views of embryos processed by ISH using a *vgll2a* probe following treatment with DMSO (control, A), SU5402 (B), DEAB (C), and RA (E). Embryos treated with 20 μM SU5402 to inhibit FGF signaling for one hour from 23–24 hpf and processed for by ISH for *vgll2a* expression show a reduction in *vgll2a* mRNA in the endodermal and ectodermal pharyngeal epithelia surrounding the arches (B, n=22/23) compared to DMSO-treated control embryos (A, n=32/34). Embryos treated from 22–23 hpf with 100 μM DEAB to inhibit RA synthesis (B, n=25/27) exhibit increased *vgll2a* expression in the pharyngeal epithelia while treatment with 100 nM all-*trans* RA (D, n=25/25) results in reduced expression of *vgll2a* in this domain. Other domains of *vgll2a* expression were not affected in these treatments (data not shown). Anterior is to the left in all panels.

$watermark-text
$watermark-text
$watermark-text

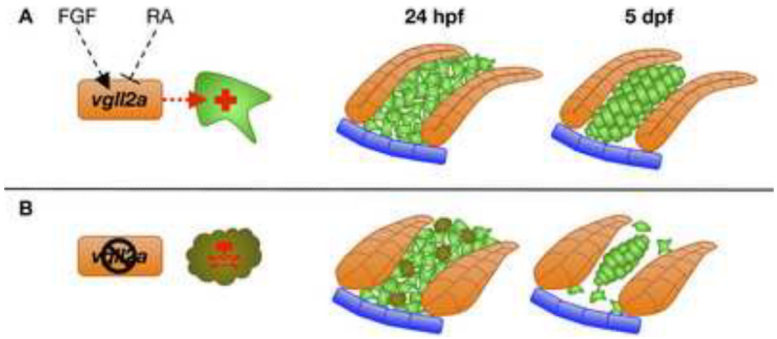

Figure 8. Model of *vgll2a* action during zebrafish craniofacial development

Model of pharyngeal cartilage development in the presence (A) and absence (B) of *vgll2a*. Expression of *vgll2a* within the pharyngeal epithelia is regulated positively by FGFs and negatively by RA (A). Within the endoderm (orange cells) and perhaps the ectoderm (blue cells), *vgll2a* regulates expression of a survival signal secreted by these epithelia and required for survival of neural crest cells (green cells) around 24 hpf. In the presence of *vgll2a* expression, these neural crest cells go on to form the pharyngeal cartilages by 5dpf. In the absence of *vgll2a* expression (B), the pharyngeal epithelia fails to express the *vgll2a*-regulated survival signal and a subset of neural crest cells undergo caspase-mediated cell death around 24 hpf. By 5 dpf, only neural crest cells in close enough association with one-another meet the critical mass required for chondrogenesis, resulting in cartilage elements that are hypoplastic or absent.

$watermark-text
$watermark-text
$watermark-text